High-Performance Computing-Enabled Computational Fluid Dynamics for Offshore Renewable Energy Fluid Machinery Development

Anna Cavazzini*, A. Sanvito⁺, M. Sergio Campobasso‡

Department of Engineering, Lancaster University, Lancaster LA1 4YR, *a.cavazzini@lancaster.ac.uk, ⁺a.sanvito@lancaster.ac.uk, ‡m.s.campobasso@lancaster.ac.uk

Introduction

Renewable Energy for electricity production plays a central role in the decarbonisation of the power sector. Wind energy has rapidly grown in the past few years supported by science and technology, opening the way to new frontiers such as floating offshore wind farms. Tidal and wave power have also a significant potential, particularly in Northern Europe, but this potential is still unexploited. To further reduce costs of wind and marine power generation, it is necessary to capture the physics of complex environmental flows and their interaction with wind and marine energy converters. High-fidelity Computational Fluid Dynamics (CFD) and High-Performance Computing have a key role in supporting further growth of Wind and Marine Energy.

RANS and *k-ω* SST equations

The time-domain (TD) Reynolds-averaged Navier-Stokes (RANS) equations coupled to Menter's shear stress transport (SST) turbulence model can be viewed as a system of integral euqations:

$$\frac{\partial}{\partial t}\left(\int_{\mathcal{C}(t)} \mathbf{U}\, d\mathcal{C}\right) + \oint_{S(t)} (\underline{\Phi}_c - \underline{\Phi}_d)\cdot d\underline{S} - \int_{\mathcal{C}(t)} \mathbf{S}\, d\mathcal{C} = 0$$

where $\mathbf{U}=[\rho\ \rho u\ \rho v\ \rho w\ \rho\varepsilon\ \rho k\ \rho\omega]$ is the vector od conserved variables, $\underline{\Phi}_c$ and $\underline{\Phi}_d$ are convective and diffusive fluxes respectively, and $\mathbf{S}$ contains turbulent and non-inertial source terms.

Our CFD codes

Finite volume structured multi-block RANS/SST codes

COSA
- **Compressible** model
- Wind turbines

ARCTIC
- **Incompressible** model
- Tidal stream turbines
- Wind turbines

Reducing CFD runtimes

Case study: two-bladed NREL Phase VI rotor in yawed wind.

Figure 1 shows COSA CFD set-up, operating regime is sketched in Fig. 2, and turbine operating conditions are given in Tab. 1.

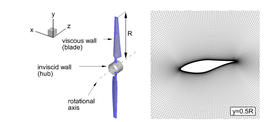

Fig. 1. NREL Phase VI HAWT CFD model

Objectives:

- Validate time domain (TD) results against measured data
- Validate frequency-domain harmonic balance (HB) results against TD data
- Assess computational time reduction achieved by using HB rather than TD analysis.

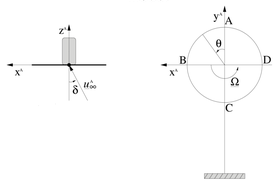

Fig. 2. Configuration for the TD and HB analysis

Wind speed	Rotational speed	Re	Yaw error
7 m/s	72 RPM	9 x 10^5	30°

Table 1. Operating conditions

Results:

- Good agreement between experimental data and TD results obtained using 360 time steps per period [6].
- Thrust and torque profiles obtained with three harmonics (HB 3) differ negligibly from the TD solution (Fig. 3).

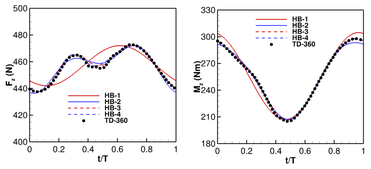

Fig. 3. Thrust and torque over a period, HB and TD results

- HB speed-up: ratio of wall-clock time of TD simulation and HB analysis with N_H harmonics. HB-3 COSA solution is 31 times faster than TD solution.

7 m/s	HB-1	HB-2	HB-3	HB-4	TD-360
Speed-up	74.7	43.6	31.0	24.0	1

Table 2. Speed-up of the HB approach

COSA HB technology has been used also for utility scale wind turbines [6].

Validation of low-fidelity methods

Case study: one-blade H-Darrieus rotor using the NACA 0021 airfoil (Fig. 5).

Objective: Validate two low-fidelity methods: Blade-Element Momentum theory (BEMT) [2] and Lifting Line Free Vortex Wake Model (LLFVW) [3] against 2D and 3D COSA CFD [2,3].

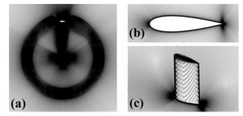

Fig. 5. one-blade H-Darrieus rotor

Results:

BEMT

- Simulations used VARDAR BEMT research code of the University of Florence, with and without considering tip flow corrections (2D BEMT).

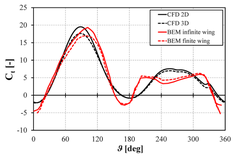

Fig. 6. Torque coefficient: CFD and BEM simulations

- Good agreement in the patterns of COSA and BEMT profiles in windward portion of revolution
- Larger differences in leeward portion (Fig. 6) [2]

LLFVW

- Torque profiles of COSA and LLFVW code of TU Berlin agree fairly well (Fig. 7) [3].

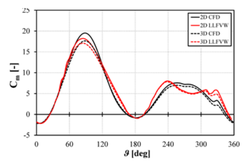

Fig. 7. Torque coefficient: CFD data and LLFVW simulations

- LLFVW gives high resolution of wakes (Fig. 10).

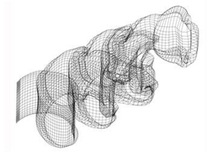

Fig. 10. Wake of LLFVW model

Floating offshore wind turbine (FOWT)

Case study: three-blade 5MW rotor (Fig. 11) in pitching FOWT mode [4] (operating conditions in Tab. 3).

Objectives:

Explore sources of uncertainty in FOWT aerodynamic design/response through the analysis of both a fixed-bottom and a pitching rotor (Fig. 12).

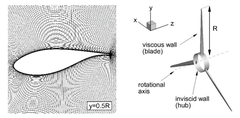

Fig. 11. NREL 5MW CFD model

Table 3. Operating conditions

Wind speed	Rotational speed	Re
11 m/s	12 RPM	7.4 x 10^6

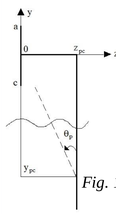

Fig. 12. FOWT pitching motion

Θ_P=4°, Ω_P=0.4π rad/s, ϕ_P=180°, y_{PC}=-90 m z_{PC}=5 m

Results:

Steady case:

- Low-speed precondition (LSP) [4] improves COSA solution (Fig. 13)

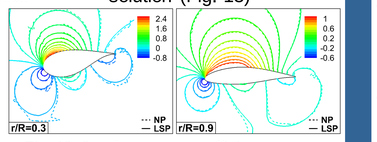

Fig. 13. Steady pressure coefficient contours, impact of using LSP

Unsteady case:

- Max. relative Mach > 0.4 at maximum tower forward speed [4] (not shown here).
- Different power and thrust peaks for COSA, FAST, and FLUENT (Fig. 14) [4].

Fig. 14. Power and thrust, COSA/FAST/FLUENT

Possible explanation:

- BEMT inadequacy to capture effects of FOWT pitching motion.
- FLUENT simulations neglect air compressibility.

Steady & Unsteady loads in tidal turbines

Case study: tidal current turbine (TCT) towing tank experiment [7].

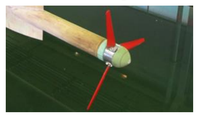

Fig. 15. TCT model [7]

Objective:

- Compare experimental data and (ANSYS FLUENT) CFD results for steady and wave-like unsteady regimes to improve design-driving knowledge.
- Develop insight into steady and unsteady TCT hydrodynamics at utility-scale, complementing knowledge achievable with low-Reynolds number tank tests.

Analysis and Results

- Steady flow: 0.45<U_∞<1.01 m/s and 67<Ω<96 RPM.
- Unsteady wave-like regime: added harmonic component to U_∞.

Fair agreement of CFD and experimental data in all cases [1].

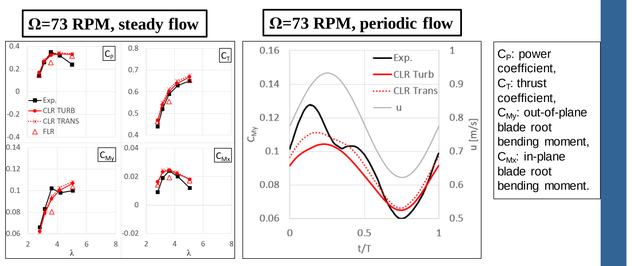

C_p: power coefficient, C_T: thrust coefficient, C_{My}: out-of-plane blade root bending moment, C_{Mx}: in-plane blade root bending moment.

Fig. 16. Measured data and CFD results [1]. Left force and power coefficients at different tip-speed ratios λ. Right: instantaneous out-of plane bending moment.

ARCTIC incompressible code

Case study: hypothetical two-blade 20 m-diameter TCT based on NREL Phase VI turbine [5].

Objectives:

- Validate ARCTIC : compare steady and unsteady incompressible analyses and compressible low-speed COSA predictions.
- Demonstrate run-time reductions of TCT wave load analysis achieved by ARCTIC HB solver.

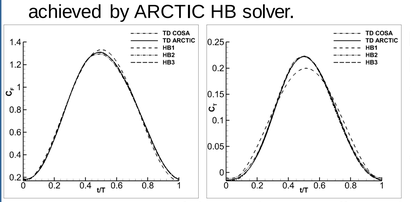

Fig. 17. Time-ariation of thrust and torque coefficients due to wave loads. COSA and ARCTIC TD and HB solutions.

Results

Figs. 17 and 18:

- TD ARCTIC and COSA analyses agree very well.
- HB-2 and TD ARCTIC solutions are in excellent agreement.

- HB-2 ARCTIC is about 9.5x faster than TD ARCTIC analysis (Tab. 4).
- incompressible TD code is about 85% faster than compressible code (Tab. 4),

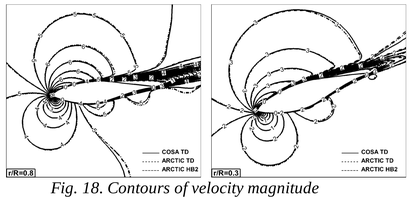

Fig. 18. Contours of velocity magnitude

offering further run-time reductions for wind turbine with negligible compressibility effects.

TD COSA	TD ARCTIC	HB-1	HB-2	HB-3
752	405	25	43	60

Table 4. CPU defined in work units (WU). 1 WU = wall-clock time for 4000 iterations of ARCTIC steady solver

Conclusions

- High Performance CFD can support the design and development of HAWTs, VAWTs and TCTs, and also validate low-fidelity methods.
- HB approach enables to obtain accurate solutions with a speed-up between 30x and 50x with respect to TD analysis.
- When compressibility effects are negligible, further computational time saving is enhanced by using incompressible CFD.

Acknowledgements

This work was supported by the UK Engineering and Physical Sciences Research Council (EPRSC) within Lancaster University Impact Acceleration Account, Grant N° . EP/R511560/1. The authors are grateful to SIMEC ATLANTIS Ltd for their advice. All ARCTIC simulations were run on the HEC cluster of Lancaster University. The authors also thank the EPRSC for providing access to computational resources on ARCHER via the UK Applied Aerodynamics Consortium Leadership Project E529.

Bibliography

[1] G. Amato, S. Doyle, S. Petley, M.S. Campobasso, I.A. Milne, and G.A. Aggidis. *Navier-Stokes CFD Analysis of a Tidal Turbine Rotor in Steady and Planar Oscillatory Flow*. In European Wave and Tidal Energy Conference, Cork, Ireland, September 2017.

[2] F. Balduzzi, J. Drofelnik, A. Bianchini, G. Ferrara, L. Ferrari, M.S. Campobasso. *Darrieus wind turbine blade unsteady aerodynamics: a threedimensional Navier-Stokes CFD assessment*. Energy 128 (2017) 550-563

[3] F. Balduzzi, D. Marten, A. Bianchini, J. Drofelnik, L. Ferrari, M.S.Campobasso, G. Pechlivanoglou, C.N. Nayeri, G. Ferrara, C.O. Paschereit, *Three-Dimensional Aerodynamic Analysis of a Darrieus Wind Turbine Blade Using Computational Fluid Dynamics and Lifting Line Theory*. Journal of Engineering for Gas Turbines and Power, February 2018, Vol. 140 / 022602-1

[4] M.S. Campobasso, A. Sanvito, A. Jackson, J. Drofelnik, Y. Zhou, Q. Xiao, and A. Croce. *Compressible Navier-Stokes analysis of floating wind turbine rotor aerodynamics*. Proceedings of IOWTC 2018 ASME 2018 1st International Offshore Wind Technical Conference November 4-7, 2018, San Francisco, CA

[5] A. Cavazzini, M.S. Campobasso. M. Marconcini, R. Pacciani, A. Arnone, *Harmonic balance Navier-Stokes analysis of tidal stream turbine wave loads*, *Recent Advances in CFD for Wind and Tidal Offshore Turbines*, Springer, to appear in May 2019.

[6] J. Drofelnik, A. Da Ronch, and M.S. Campobasso. *Harmonic balance Navier-Stokes aerodynamic analysis of horizontal axis wind turbines in yawed wind*. Wind Energy, 21(7):515–530, 2018. DOI: 10.1002/we.2175.

[7] I.A. Milne, A.H. Day, R.N. Sharma, R.G.J. Flay, *Blade loads on tidal turbines in planar oscillatory flow*, Ocean Eng., 60: 163-174, 2013.